Spontaneous spin-polarized current in a nonuniform Rashba interaction system

Qing-feng Sun[1,*] and X. C. Xie[2,3,1]

[1] *Beijing National Lab for Condensed Matter Physics and Institute of Physics, Chinese Academy of Sciences, Beijing 100080, China*

[2] *Department of Physics, Oklahoma State University, Stillwater, Oklahoma 74078*

[3] *International Center for Quantum structures, Chinese Academy of Sciences, Beijing 100080, China*

(Dated: February 2, 2008)

We investigate the electron transport through a two-dimensional semiconductor with a nonuniform Rashba spin-orbit interaction. Due to the combination of the coherence effect and the Rashba interaction, a spontaneous spin-polarized current emerges in the absence of any magnetic material and magnetic field. For a two-terminal device, only the local current contains polarization; however, with a four-terminal setup, a polarized total current is produced. This phenomenon may offer a novel way for generating a spin-polarized current, replacing the traditional spin-injection method.

PACS numbers: 72.25.-b, 73.21.Hb, 75.47.-m

How to generate the spin-polarized current in a semiconductor (SC) has been one of the most significant and challenging issues in condensed matter physics.[1,2,3] Apart from the fundamental physics interest, it may also have direct commercial applications. Over the past several years, the issue has attracted great experimental and theoretical efforts. Due to the fact that semiconductors are in general spin-unpolarized, the key for generating polarized current in previous works is through spin injection, namely, to produce spin-polarized electrons from a polarized source [e.g. Ferromagnet (FM) or polarized photon], then inject them into a SC. However, among the currently existing spin injection methods,[1,3] none is very satisfactory. For the spin injection from a FM to a SC, its spin-polarization efficiency is usually low with a typical polarization around 1%.[4] For the polarized optical methods of spin injection, it is difficult for the integration with electronic devices.[5]

Very recently, based on the Rashba spin-orbit (SO) interaction, some theoretical works have proposed different approaches to generate a spin-polarized current without FM materials.[6,7,8] However their devices are usually complicated or an external magnetic field is required. The Rashba SO interaction is an intrinsic interaction in a two-dimensional electron system (2DES) of SC heterostructures.[9,10] It originates from an asymmetrical interface electric field, i.e. the asymmetrical potential energy in the direction perpendicular to the interface. The strength of the Rashba interaction can be tuned and controlled by an external electric-field or gate voltage.[11]

In this paper, we predict that a spin-polarized current spontaneously emerges in the SC in the presence of a nonuniform Rashba SO interaction. In particular, this spin-polarized current is an intrinsic property of the nonuniform Rashba's SC and it does not need any magnetic materials nor a magnetic field. While under a voltage bias, a local polarized current is produced everywhere, but with zero total polarized current. However, if for an open multi-terminal setup, a total polarized current emerges. Thus, our proposal offers an efficient and simple method to generate the spin-polarized current.

We first show the principle of generating a spin-polarized current. For simplicity, we assume two paths for an electron traveling from one terminal of the sample to the other (see Fig.1a), and t_1 and t_2 are their respective transmission coefficients. Because the Rashba interaction strength α is tunable in experiments,[11] we choose different α in the two paths. An extreme case is $\alpha = 0$ in one path, e.g., path-1, and a large α in the path-2. This particular choice is not essential, but it brings out the physics more clearly. Due to the Rashba interaction, an extra phase is generated when an electron passes the path-2.[12] In particular, this phase is dependent on the spin of the incident electron. For a spin-up electron, the extra phase is $\varphi = -k_R L = -\alpha m^* L/\hbar^2$ (where L is the length of the path-2 and m^* is the electron effective mass), assuming the Rashba energy is weak compared with the kinetic energy. On the other hand, the phase is $-\varphi = k_R L$ for a spin-down electron. If only to consider the first-order tunneling process, the total transmission probability for the spin-up incident electron is $T_\uparrow = |t_1 + t_2 e^{i\varphi}|^2$, which in general is different from that for the spin-down electron, $T_\downarrow = |t_1 + t_2 e^{-i\varphi}|^2$. Therefore, a spin-polarized current is spontaneously generated and its polarization p at zero temperature is:

$$p = \frac{T_\uparrow - T_\downarrow}{T_\uparrow + T_\downarrow} = \frac{2|t_1 t_2| \sin\theta \sin\varphi}{|t_1|^2 + |t_2|^2 + 2|t_1 t_2| \cos\theta \cos\varphi}, \quad (1)$$

where θ is the phase difference between t_1 and t_2.

Next, we consider a specific two-dimensional and two-terminal SC system, shown in Fig.1c. In this device, two wires, II and III, are in the center region. In order to show our results are general, we choose the system without the mirror symmetry. In this set-up, an incident electron from Terminal I traveling to Terminal IV has two paths, i.e. passing the region II or III. If the Rashba interaction α's are different in the regions II and III, the above-mentioned coherent effect will occur. Then a spin-polarized current should be generated, although there is no magnetic material nor a magnetic field.

The Hamiltonian for the two-terminal system (Fig.1c)

is:

$$H = \frac{p_x^2 + p_z^2}{2m} + V(x,z) + \frac{\alpha}{\hbar}(\sigma_z p_x - \sigma_x p_z), \qquad (2)$$

where $V(x,z)$ is the potential energy. Here we let $V(x,z) = 0$ in the region I and IV; $V(x,z) = V_2$ (or V_3) in the region II (or III); and $V(x,z) = \infty$ in other regions. The last term in Eq.[2] is the Rashba interaction and $\alpha(x,z)$ describes its strength. For simplicity, we assume that $\alpha = 0$ in the regions I and IV, and $\alpha = \alpha_2$ and α_3 in the regions II and III. Boundary matching is employed to solve for the transmission coefficients.[13,14] Assuming that the incident electron is at the subband n with the spin index s and the energy E from Terminal I, and to neglect the mixing of the inter-subband in the regions II and III,[12,15] the wave functions $\Phi(x,z)$ in the regions I to IV are written as follows:[15]

$$\Phi(x,z) = \begin{cases} e^{ik_n^I x}\varphi_n^I(z)s + \sum_m r_{mns} e^{-ik_m^I x}\varphi_m^I(z)s \\ \sum_m a_{mns}^+ e^{ik_{ms}^{II+} x}\varphi_m^{II}(z)s + \sum_m a_{mns}^- e^{ik_{ms}^{II-} x}\varphi_m^{II}(z)s \\ \sum_m b_{mns}^+ e^{ik_{ms}^{III+} x}\varphi_m^{III}(z)s + \sum_m b_{mns}^- e^{ik_{ms}^{III-} x}\varphi_m^{III}(z)s \\ \sum_m t_{mns} e^{ik_m^{IV} x}\varphi_m^{IV}(z)s \end{cases}$$

$s = \uparrow / \downarrow$ is the spin index, and s also describes the corresponding spin states, in which $s = (1,0)^T$ for $\uparrow$ and $s = (0,1)^T$ for $\downarrow$. $\varphi_m^\beta(z)$ (β = I, II, III, and IV) is orthonormal transverse wave functions for the subband m in the region β. $k_m^{I/IV}$ and $k_{ms}^{\gamma\pm}$ (γ = II or III) are the corresponding x-direction wave vectors with $k_m^{I/IV} = \sqrt{\frac{2m^*}{\hbar^2}(E - E_m^{I/IV})}$ and $k_{ms}^{\gamma\pm} = \pm\sqrt{\frac{2m^*}{\hbar^2}(E - V_\gamma - E_m^\gamma) + k_{R\gamma}^2} - sk_{R\gamma}$, in which $k_{R\gamma} \equiv \alpha_\gamma m^*/\hbar^2$ and $E_m^\beta = \frac{\hbar^2}{2m^*}(\frac{m\pi}{W^\beta})^2$. t_{mns} and r_{mns} are the transmission and reflection amplitudes; $a_{mns}^\pm$ and $b_{mns}^\pm$ are constants to be determined by matching the boundary conditions. Here the boundary conditions are:[16,17] $\Phi(x,z)|_{x=0^-/L^-} = \Phi(x,z)|_{x=0^+/L^+}$ and $\hat{v}_x\Phi(x,z)|_{x=0^-/L^-} = \hat{v}_x\Phi(x,z)|_{x=0^+/L^+} + \frac{2iU_0}{\hbar}\Phi(0/L,z)$, where $\hat{v}_x = (p_x + \sigma_z\hbar k_R)/m^*$ is the velocity operator and U_0 is the Schottky δ barrier potentials at the interfaces.[18] Using the above boundary conditions, t_{mns} can be exactly obtained, including all orders of reflection and tunnelling processes. After solving t_{mns}, the transmission probability T_s can be obtained through the relation $T_s(E) = \sum_{m,n}\theta(E - E_n^I)\theta(E - E_m^{IV})\frac{k_m^{IV}}{k_n^I}|t_{mns}|^2$. Similarly, the current (or conductance) density at an arbitrary location (x,z) can also be obtained. For instance, the conductance density $g_{Xs}(x,z)$ in the x-direction in the region IV is:

$$g_{Xs}(x,z) = \frac{dj_{Xs}}{dV} = \frac{e^2}{h}\int dE \frac{-\partial f(E)}{\partial E}\sum_n \frac{1}{k_n} Re\left[\sum_m t_{mns}^* e^{-ik_m^{IV*}x}\varphi_m^{IV*}(z)\right]\left[\sum_m t_{mns} k_m^{IV} e^{ik_m^{IV}x}\varphi_m^{IV}(z)\right] \qquad (3)$$

where $f(E) = 1/[exp^{(E-E_F)/k_B\mathcal{T}} + 1]$ is the Fermi distribution function with E_F being the Fermi energy.

We numerically study the conductance density $g_{Xs}(x,z)$ and the local spin polarization $p(x,z) \equiv [g_{X\uparrow} - g_{X\downarrow}]/[g_{X\uparrow} + g_{X\downarrow}]$. In the numerical calculations, we choose the system sizes to be: $W_L = W_R = L = 100nm$, $W_{sd} = W_N = 30nm$, $a_L = 0$, $a_R = 30nm$, and $D = 10nm$. We also set $k_{R3} = 0$ and $k_{R2} = 0.015/nm$, with the corresponding $\alpha_2 = \frac{\hbar^2 k_{R2}}{m^*} \approx 3\times 10^{-11} eVm$ for $m^* = 0.036m_e$. Fig.2 shows $p(x,z)$ in the region IV. Here $p(x,z)$ is clearly non-zero, and it can be over 15% at some locations. This means that the coherent effect as shown in Fig.1a indeed plays the role for a finite $p(x,z)$. For a further verification, we also study the following two cases for which the coherent effect is expected to vanish: (i) closing one channel, e.g. to make the region III to be very narrow; (ii) to set the α to be equal in both regions II and III (i.e. to set $\alpha_2 = \alpha_3$). Indeed, we find $p(x,z) = 0$ in both cases for any (x,z).

Now we show the behavior of the local spin polarization $p(x,z)$ in detail by plotting $p(x,z)$ (the red dotted curve in Fig.3c) and the corresponding conductance density $g_{X\uparrow/\downarrow}$ (see Fig.3a) versus z at $x = 100nm$, i.e. the dotted line position in Fig.2. Fig.3a exhibits that $g_{X\uparrow}$ and $g_{X\downarrow}$ have clear difference. In particularly, at the peak position of $g_{X\uparrow/\downarrow}$ this difference remains, and it even reaches the largest value. Moreover the total conductance $G_s = \int dz g_{Xs}(x,z)$ is quite large, (e.g. $G_\uparrow = G_\downarrow \approx 1.2e^2/h$ for the parameters of Fig.2 and Fig.3a,b). This means that this system can generate a large current density with a large local spin polarization. More importantly, the above property always survives, so long as the system size is within the coherent length. For example, at $x = 1000nm$, $g_{X\uparrow}$ and $g_{X\downarrow}$ still have large difference (see Fig.3b) and $p(x,z)$ can exceed $\pm 10\%$ in a wide range of z (see the red dotted curve in Fig.3d).

Next we investigate how the local spin polarization $p(x,z)$ depends on sample parameters. (i) When the potential V_3 varies slightly, $p(x,z)$ changes substantially. It can vary from the largest positive value to the largest negative value and vice versa (see Fig.3c). This characteristic is very useful. Because V_3 can be controlled by a gate voltage, so $p(x,z)$ can also be tuned and controlled in an experiment. (ii) If there exists an interface potential U_0, $p(x,z)$ is barely affected. It may still exceed 10% (see the blue dash-dotted curve in Fig.3d). But the conductances G_s and g_{Xs} are weakened by a large U_0. (iii) With an increased distance D between the two channels, the overlap of two outgoing waves from the two channels is smaller, so $p(x,z)$ will reduce slightly (see the black solid curve in Fig.3d). But $|p(x,z)|$ can still exceed 5% for $D = 50nm$. (iv) With a larger Fermi energy E_F, more subbands in the region I-IV are available that increases G_s and g_{Xs}. Meanwhile the variation of $p(x,z)$ versus z exhibits a stronger oscillation, and its amplitude decreases slightly (see the magenta dashed curve in Fig.3d).

We emphasize although the local spin polarization

$p(x,z)$ is fairly large almost everywhere,[19] the total conductance G_s is unpolarization (i.e. $G_\uparrow = G_\downarrow$) for any two-terminal devices, because the two-terminal AB setup has the phase-locking effect.[20] We prove the above statement in detail below. Due to the current conservation and the time-reversal invariance, the transmission coefficient for a two-terminal AB system without the spin degrees of freedom has the property of $T(E,\phi) = T(E,-\phi)$, the so called "phase-locking effect", where ϕ is the magnetic flux through the AB loop.[20] In our system, since no spin-flip process,[12,15] the spin-up and spin-down electrons can be treated as two independent sub-systems. In the spin-up system, when an electron passes the lower channel, an extra phase $\varphi = -k_{R2}L$ is added because of the Rashba interaction.[12] This extra phase plays the same role as if an external magnetic flux thread the AB loop. Then we have $T_\uparrow(E) = T(E,\varphi)$. Similarly, for the spin-down system, a fictitious magnetic flux $-\varphi$ appears, and $T_\downarrow = T(E,-\varphi)$. Therefore, $T_\uparrow(E) = T_\downarrow(E)$ and $G_s = \frac{e^2}{h}\int dE \frac{-\partial f(E)}{\partial E} T_s(E)$ must be spin-unpolarization, i.e. $G_\uparrow = G_\downarrow$ for any two-terminal devices.

In order to obtain a polarized total conductance (or current), we devote the rest of the paper to study four-terminal devices. Consider a specific four-terminal device as shown in Fig.1d, in which the right (outgoing) terminal (the original region IV) is splitted into three terminals at the position $x = L + L_2$. Assuming an incident electron from Terminal I, the wave function $\Phi(x,z)$ in the region I-VII (see Fig.1d) can be written similarly as for the two-terminal case. By matching boundary conditions at $x = 0$, L, and $L + L_2$, the transmission amplitudes $t^\beta_{mns}(E)$ (β = V, VI, and VII) from the nth subband of Terminal I to the mth subband of Terminal β can be exactly obtained, although the deductive process is more complicated here. Afterwards, the transmission probability $T^\beta_s(E) = \sum_{m,n}\theta(E - E^I_n)\theta(E - E^\beta_m)\frac{k^\beta_m}{k^I_n}|t^\beta_{mns}|^2$ and the conductance $G^\beta_s = \frac{e^2}{h}\int dE \frac{-\partial f(E)}{\partial E} T^\beta_s(E)$ can also be calculated. In the numerical calculations, we choose the device geometry as: The left side and the center region II and III are the same as for the two-terminal device, and the sizes on the right are $a_R = 50nm$, $W_5 = W_7 = 50nm$, $W_6 = 30nm$, $W_R = 200nm$, and $L_2 = 100nm$ (see Fig.1d). To simplify, we set the potential energy V and the Rashba interaction α in the region I, IV, V, VI, and VII to be zero. In a multi-terminal device, the total conductance G^β_s and the total current are spin polarized, so we focus on G^β_s and its polarization p^β [$p^\beta \equiv (G^\beta_\uparrow - G^\beta_\downarrow)/(G^\beta_\uparrow + G^\beta_\downarrow)$], instead of the local conductance $g_{Xs}(x,z)$ and the local polarization $p(x,z)$ as in the two-terminal case.

Fig.4a and 4b show the conductance G^{VI}_s and its polarization p^{VI} versus the potential V_3. $G^{VI}_\uparrow$ and $G^{VI}_\downarrow$ show a large difference. This difference can be more than $0.15e^2/h$ and p^{VI} can exceed $\pm 10\%$ in a wide range of V_3. p^{VI} versus V_3 exhibits an oscillatory behavior. In particular, it can oscillate from a maximum positive (or negative) value to a maximum negative (or positive) value with changing V_3. This characteristic is very useful, meaning that the spin-polarized direction and strength can be conveniently controlled in an experiment by tuning the potential V_3. For the other two terminals V and VII, $G^{V/VII}_s$ and $p^{V/VII}$ have similar behaviors. Below we emphasize two points: (i) It is the total conductance (or current) that is polarized, not only the conductance density with local polarization. This polarization can survive within the spin coherent length instead of the electron coherent length as in the two-terminal case. Usually, the former may be much longer than the latter.[21] (ii) In the present device, the spin-polarized current is generated without any magnetic material or a magnetic field. In the zero bias case, anywhere inside the sample is nonmagnetic. When a bias is added, a spin-polarized current spontaneously emerges due to the coherent effect and a nonuniform Rashba interaction.

We now study how the polarization p^{VI} depends on other parameters: (i) p^{VI} versus the Fermi energy E_F exhibits disorder-like oscillating behavior, and the amplitude slightly weakens at high E_F (see Fig.4c). (ii) p^{VI} versus k_{R2} (i.e., α_2) is sinusoid-like curve with the period $\sim 2\pi$ (Fig.4d). But it is not exact periodic function because the Rashba interaction also gives rise to an energy term $\hbar^2 k^2_R/2m^*$ except for the extra phase $-\sigma k_R L$. (iii) Fig.4e shows p^{VI} versus k_{R3} (i.e., α_3). Clearly $k_{R3} = 0$ is not essential for a non-zero p^{VI}. As long as $|k_{R3} - k_{R2}| \neq 0$, a spin-polarized current appears.

Finally, let us discuss the realizability. To add a gate (the deep gray region in Fig.1b) in a SC 2DGS, one can make the Rashba interaction α in this region different from the α's in other regions.[11] Then under a bias, a local spin-polarized current is automatically induced. If four extra split gates (the black one in Fig.1b) are added to form an open multi-terminal device, a total spin-polarized current is generated from source to drain. Notice that the device of Fig.1b has been realized about 15 years ago.[22] Moreover, this device is much more open than the above-mentioned four-terminal device (Fig.1d). The phase-locking effect is more severely destroyed, hence, this kind of set-up will have a much larger p. In fact, if the system is sufficiently open, then only the first-order tunneling process exists due to the current bypass effect, the spin-polarization p can reach 100% at $|t_1| = |t_2|$ and $\theta = \varphi = \pi/2$ [see Eq.(1)].

In summary, we propose a new method for generating the spin-polarized current, replacing the traditional spin-injection approach. Here the spin-polarized current is induced due to the combination of the quantum coherent effect and the Rashba spin-orbit interaction. In the two-terminal device, a local spin-polarized current is produced. While in an open multi-terminal setup, a total spin-polarized current emerges in the absence of any magnetic material or an external magnetic field.

Acknowledgments: We gratefully acknowledge financial support from the Chinese Academy of Sciences and NSFC under Grant No. 90303016 and No. 10474125. XCX is supported by US-DOE under Grant

No. DE-FG02-04ER46124 and NSF-MRSEC under DMR-0080054.

*Electronic address: sunqf@aphy.iphy.ac.cn

[1] S.A. Wolf, D.D. Awschalom, R.A. Buhrman, J.M. Daughton, S.V. Molnar, M.L. Roukes, A.Y. Chtchelkanova, and D.M. Treger, Science **294**, 1488 (2001).

[2] G.A. Prinz, Science **282**, 1660 (1998).

[3] I. Zutic, J. Fabian, and S. Das Sarma, Rev. Mod. Phys. **76**, 323 (2004).

[4] G. Schmidt, D. Ferrand, L.W. Molenkamp, A.T. Filip, and B.J.V. Wees, Phys. Rev. B **62**, 4790 (2000); P.C. van Son, H. van Kempen, P. Wyder, Phys. Rev. Lett. **58**, 2271 (1987).

[5] I. Zutic, J. Fabian, and S. Das Sarma, Appl. Phys. Lett. **79**, 1558 (2001); **82**, 221 (2003).

[6] R. Ionicioiu and I. D'Amico, Phys. Rev. B **67** 041307(R) (2003).

[7] V.M. Ramaglia, D. Bercioux, V. Cataudella, G. De Filippis, C.A. Perroni, and F. Ventriglia, Eur. Phys. J. B **36**, 365 (2003).

[8] A.A. Kiselev and K.W. Kim, J. Appl. Phys. **94**, 4001 (2003).

[9] E.I. Rashba, Fiz. Tverd. Tela (Leningrad) **2**, 1224 (1960) [Solid State Ionics **2**, 1109 (1960)].

[10] Y.A. Bychkov and E.I. Rashba, J. Phys. C **17**, 6039 (1984).

[11] J. Nitta, T. Akazaki, H. Takayanagi, and T. Enoki, Phys. Rev. Lett. **78**, 1335 (1997); T. Matsuyama, R. Kursten, C. Meibner, and U. Merkt, Phys. Rev. B **61**, 15588 (2000).

[12] S. Datta and B. Das, Appl. Phys. Lett. **56**, 665 (1990).

[13] R. Shankar, *Principles of Quantum Mechanics* (Plenum Press, New York, 1980), p177.

[14] R.L. Schult, D.G. Ravenhall, and H.W. Wyld, Phys. Rev. B **39**, 5476 (1989); J. Wang, H. Guo, and R. Harris, Appl. Phys. Lett. **59**, 3075 (1991); Q.F. Sun, P. Yang, and H. Guo, Phys. Rev. Lett. **89**, 175901 (2002).

[15] When the mixture of the inter-subband is neglected, σ_z is a good quantum number and the spin-flip process will not occur, so there are no terms with the spin $-s$ in the wave function $\Phi(x,z)$. If $k_R^2 W_s^2 \ll 1$, the above approximation is quite reasonable. For example, see M.H. Larsen, A.M. Lunde, and K. Flensberg, Phys. Rev. B **66**, 033304 (2002).

[16] Here the boundary conditions require the continuity of the velocity operator acting on the wave function instead of the derivative continuity, because $p_x\alpha(x) = \alpha(x)p_x - i\hbar\frac{\partial}{\partial x}[\alpha(x)]$ and $\alpha(x)$ is not continuous at the interface. For example, see L.W. Molenkamp, G. Schmidt, and G.E.W. Bauer, Phys. Rev. B **64**, 121202 (2001); U. Zulicke and C. Schroll, Phys. Rev. Lett. **88**, 029701 (2002).

[17] A. Szafer and A.D. Stone, Phys. Rev. Lett. **62**, 300 (1989).

[18] F. Mireles and G. Kirczenow, Phys. Rev. B **66**, 214415 (2002).

[19] In fact, in the incident region I and the middle region II and III, the local currents also are spin-polarization.

[20] M. Buttiker, Phys. Rev. Lett. **57**, 1761 (1986); G. Hackenbroich, Phys. Rep. **343**, 463 (2001).

[21] J.M. Kikkawa and D.D. Awschalom, Phys. Rev. Lett. **80**, 4313 (1998); R.M. Potok, J.A. Folk, C.M. Marcus, and V. Umansky, *ibid.* **89**, 266602 (2002).

[22] For example, see U. Meirav, M.A. Kastner, and S.J. Wind, Phys. Rev. Lett. **65**, 771 (1990).

FIG. 1: (Color online) (a) Schematic diagram for an electron transport through two paths in a two-terminal device. (b) Schematic diagram for an open multi-terminal device made of semiconductor 2DGS with four split gates (the black region). The Rashba interaction in the deep gray region differs from the rest of the system. (c) and (d) are the configurations for the specific two-terminal and four-terminal systems, respectively.

FIG. 2: (Color online) The local spin polarization $p(x,z)$ vs x,z in the region IV for the two-terminal device. The parameters are $V_2 = 0$, $V_3 = -0.02eV$, $E_F = 0.013eV$, $U \equiv \frac{2m^*U_0}{\hbar^2} = 0$, and $k_B\mathcal{T} = 0$.

FIG. 3: (Color online) (a) and (b), $g_{X\uparrow}$ (solid) and $g_{X\downarrow}$ (dotted) vs. z for $x = 100nm$ (in a) and $x = 1000nm$ (in b). (c) $p(x,z)$ vs z for $V_3 = -0.023$, -0.02(the red dotted curve), -0.026, -0.028, and -0.031eV along the arrow direction. (d) $p(x,z)$ vs z for the cases of (i) $x = 1000nm$ (red dotted curve); (ii) $U = 0.2/nm$ (blue dash-dotted curve); (iii) $D = 20nm$ and $a_R = 20nm$ (black solid curve); (iv) $E_F = 0.05$eV (magenta dashed curve). The others no-mentioned parameters in (a), (b), (c), and (d) are the same as for Fig.2 and at $x = 100nm$.

FIG. 4: (Color online) (a) $G_\uparrow^{VI}$ (solid) and $G_\downarrow^{VI}$ (dotted) vs V_3. (b) p^{VI} vs V_3 for $E_F = 0.013eV$ (solid) and $0.015eV$ (dotted). (c) p^{VI} vs E_F. (d) p^{VI} vs k_{R2} for $E_F = 0.013eV$ (solid) and $0.015eV$ (dotted). (e) p^{VI} vs k_{R3} for $k_{R2} = 0.015/nm$ (solid) and $k_{R2} = 0.03/nm$ (dotted). The other non-mentioned parameters in (a)-(e) are $V_2 = 0$, $V_3 = -0.02eV$, $k_{R2} = 0.015/nm$, $k_{R3} = 0$, and $E_F = 0.013eV$.

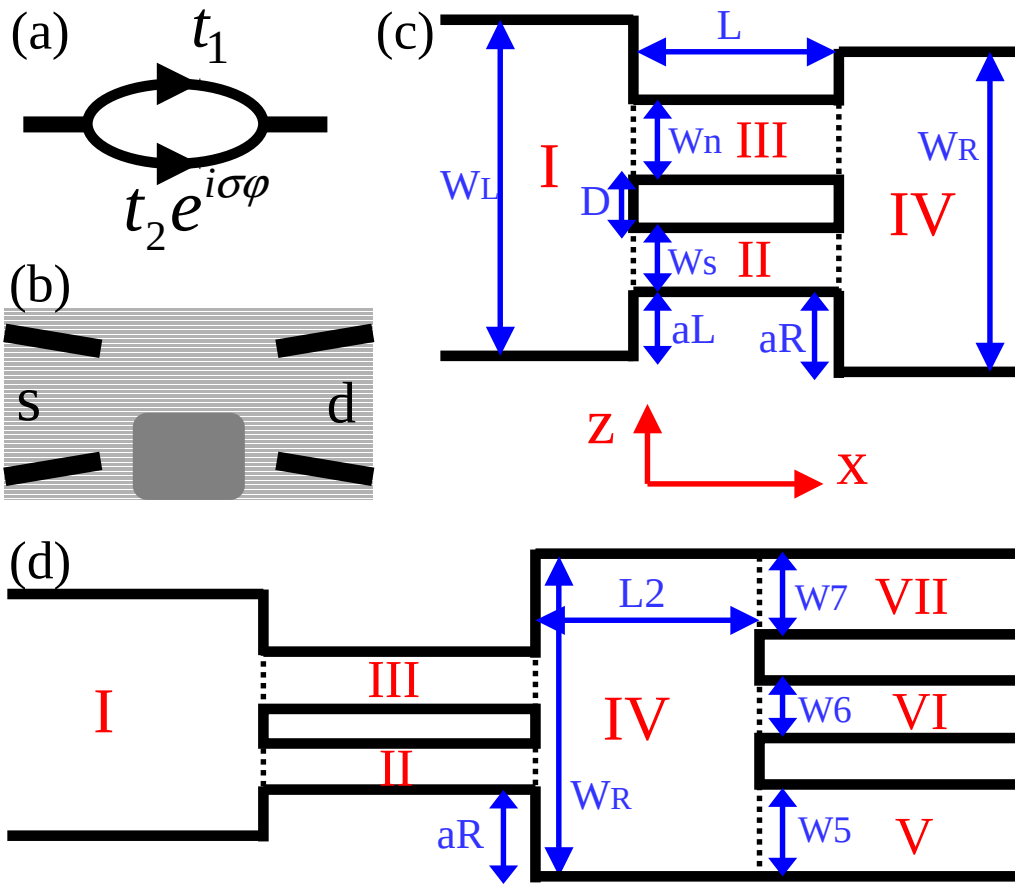
(a)
t_1
$t_2 e^{i\sigma\varphi}$
(b)
s
d
(c)
L
W_L
I
Wn
III
D
Ws
II
W_R
IV
aL
aR
z
x
(d)
I
III
II
IV
L2
W7
VII
W6
VI
W5
V
aR
W_R

Fig.1

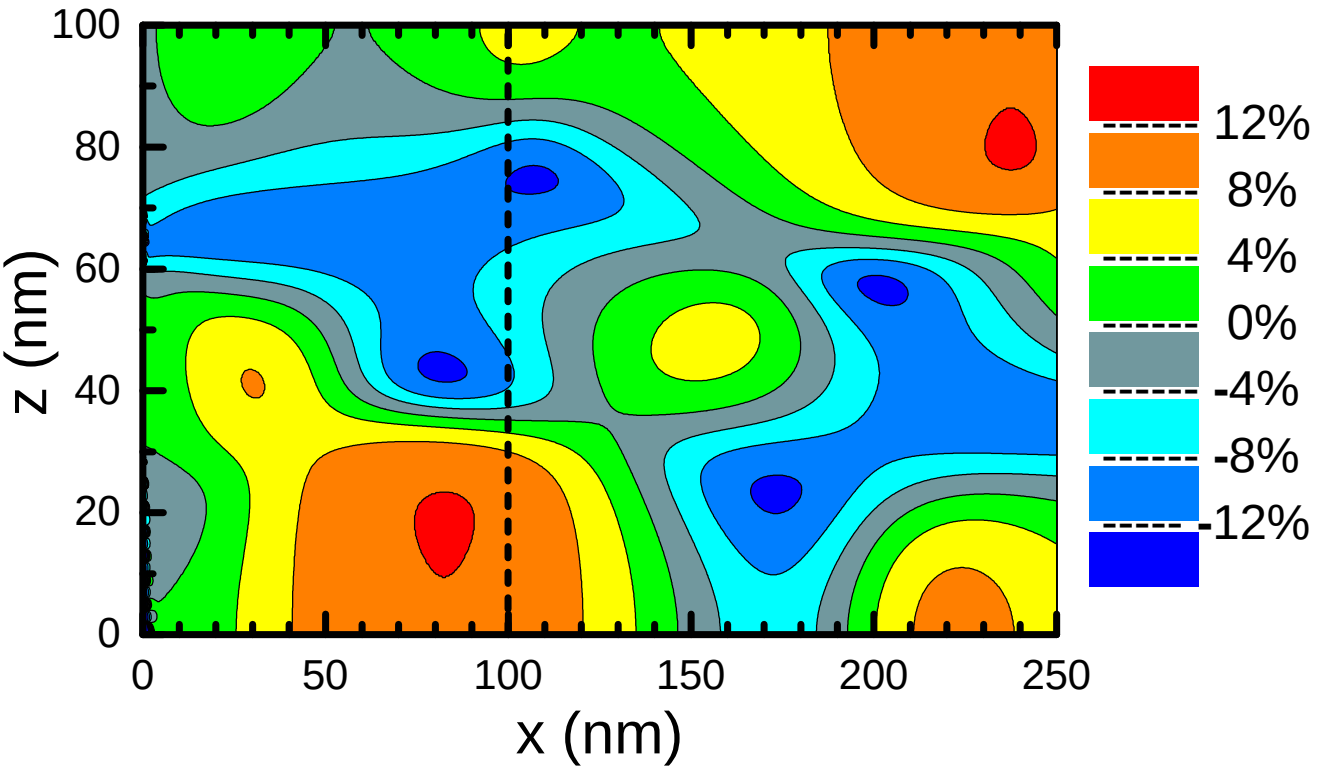

Fig.2

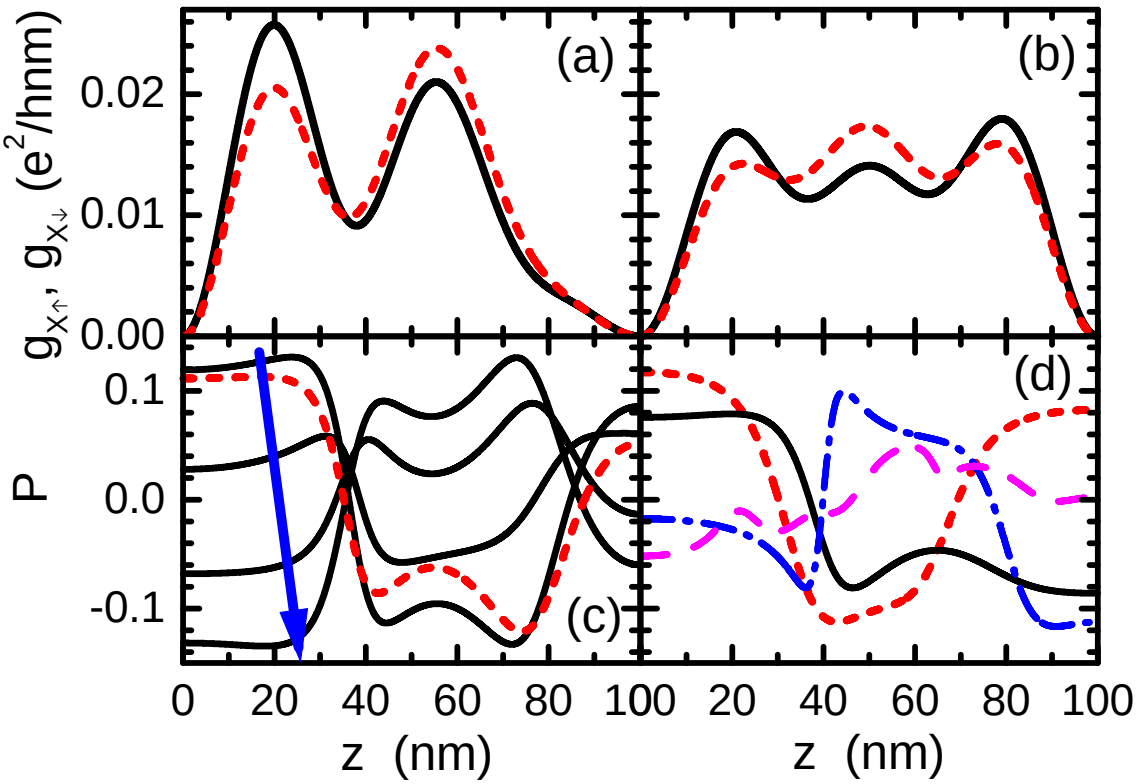
(a)
(b)
(c)
(d)
0.02
0.01
0.00
0.1
0.0
-0.1
P
$g_{X\uparrow}$, $g_{X\downarrow}$ (e^2/hnm)
0
20
40
60
80
100
z (nm)

Fig.3

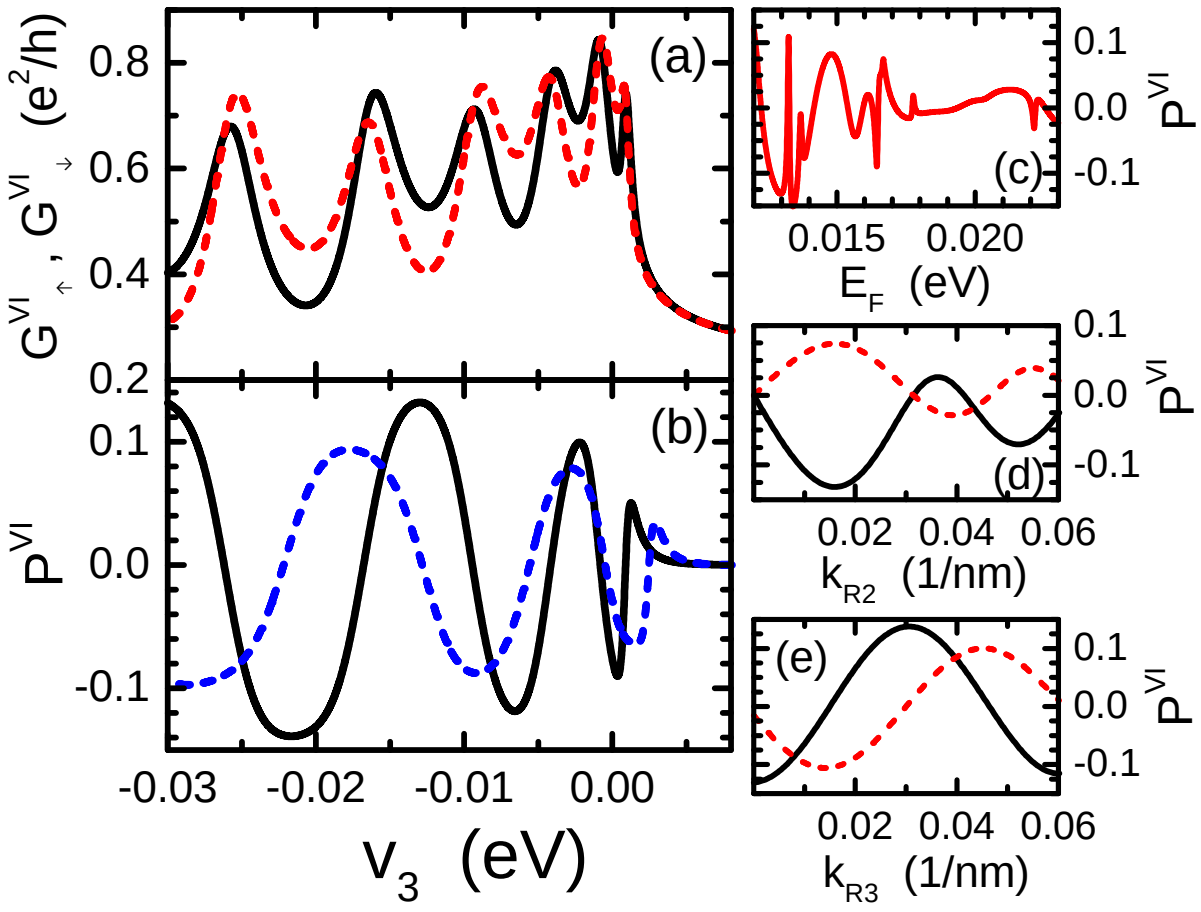
(a)
(b)
(c)
(d)
(e)
$G^{VI}_{\uparrow}, G^{VI}_{\downarrow}$ (e^2/h)
P^{VI}
v_3 (eV)
E_F (eV)
k_{R2} (1/nm)
k_{R3} (1/nm)

Fig.4